Langmuir
The ACS Journal of Surfaces and Colloids

MAY 8, 2007
VOLUME 23, NUMBER 10

Letters

Protein Crystallization at the Air/Water Interface Induced by Shearing Bulk Flow

Ali N. Azadani,[†] Juan M. Lopez,[‡] and Amir H. Hirsa*[,†]

Department of Mechanical, Aerospace and Nuclear Engineering, Rensselaer Polytechnic Institute, Troy, New York 12180, and Department of Mathematics and Statistics, Arizona State University, Tempe, Arizona 85287

Received November 3, 2006. In Final Form: December 12, 2006

We have observed 2D protein crystallization under conditions where in the absence of flow, crystallization fails to occur. Even under conditions where crystallization does occur in quiescent systems, we have found that flow can accelerate the crystallization process. By interrogating the flow responsible for this enhanced crystallization, we have correlated the enhancement with large shear in the plane of the interface. Some possible mechanisms for why interfacial shear can enhance the crystallization process are proposed.

The ability to utilize detailed knowledge of the structure of proteins and to define their interactions with ligands has enabled many advances in our understanding of biological systems and the rational design of new drugs and pharmacological agents. The primary technique that yields a detailed description of protein structure is X-ray diffraction analysis. A major challenge to the full exploitation of this powerful technique is that the protein must first be crystallized. The basis of protein crystallization is that a protein solution must by some means be transformed to a supersaturated state whereby its return to equilibrium forces the exclusion of protein from the solution and into a solid phase (i.e., the crystal).

In contrast to growing 3D protein crystals in the bulk, 2D protein crystallization greatly simplifies both the theoretical and experimental aspects of protein studies. In addition, 2D systems are not affected by gravity, an issue that plagues 3D crystallographers. Two-dimensional protein crystallization on lipid monolayers at the air/water interface (in quiescent systems) is a well-established technique.[1,2] The most commonly used approach entails the specific binding of a protein to a ligand-embedded lipid monolayer. The protein crystallized most extensively is the bacterial protein streptavidin, which is a well-characterized protein with a high binding affinity to biotin.[3−5] Several studies have found that streptavidin can be crystallized on a biotinylated lipid monolayer.[2,6−12] The dissolved streptavidin in the bulk liquid binds to the ligands formed by the insoluble biotinylated lipid monolayer initially spread on the liquid surface. By virtue of a high concentration of protein at the interface and the fluidity of the monolayer, the protein self-assembles into the crystal form.

* Corresponding author. E-mail: hirsaa@rpi.edu.
[†] Rensselaer Polytechnic Institute.
[‡] Arizona State University.

(1) Blankenburg, R.; Meller, P.; Ringsdorf, H.; Salesse, C. *Biochemistry* **1989**, *28*, 8214−8221.
(2) Darst, A. A.; Ahlers, M.; Meller, P. H.; Kubalek, E. W.; Blankenburg, R.; Ribi, H. O.; Ringsdorf, H.; Kornberg, R. D. *Biophys. J.* **1991**, *59*, 387−396.
(3) Chaiet, L.; Wolf, F. J. *Arch. Biochem. Biophys.* **1964**, *106*, 1−5.
(4) Green, N. M. *Methods Enzymol.* **1990**, *184*, 51−67.
(5) Bayer, E. A.; Ben-Hur, H.; Wilcheck, M. *Methods Enzymol.* **1990**, *184*, 217−233.
(6) Haas, A.; Brezesinski, G.; Möhwald, H. *Biophys. J.* **1995**, *68*, 312−314.
(7) Vénien-Bryan, C.; Lenne, P.-F.; Zakri, C.; Reault, A.; Brisson, A.; Legrand, J.-F.; Berge, B. *Biophys. J.* **1998**, *74*, 2649−2657.
(8) Hemming, S. A.; Bochkarev, A.; Darst, S. A.; Kornberg, R. D.; Ala, P.; Yang, D. S. C.; Edwards, A. M. *J. Mol. Biol.* **1995**, *246*, 308−316.
(9) Frey, W.; Schief, W. R.; Vogel, V. *Langmuir* **1996**, *12*, 1312−1320.
(10) Wang, S.-W.; Robertson, C. R.; Gast, A. P. *J. Phys. Chem. B* **1999**, *103*, 7751−7761.
(11) Edwards, T. C.; Malmastadt, N.; Koppenol, S.; Masahiko, H.; Vogel, V.; Stayton, P. S. *Langmuir* **2002**, *18*, 7447−7451.
(12) Ratanabanangkoon, P.; Gast, A. P. *Langmuir* **2003**, *19*, 1794−1801.

10.1021/la063223x CCC: $37.00
Published on Web 04/03/2007

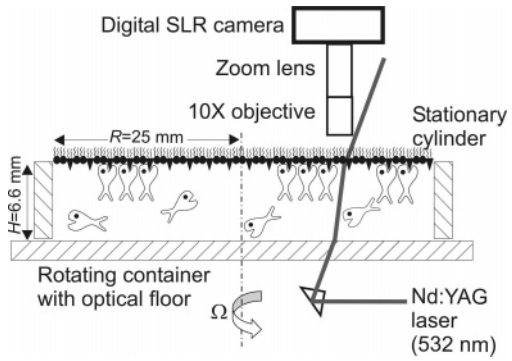

Figure 1. Schematic of the experimental setup. The protein crystals (and/or clusters) are illuminated by forward scattering of a laser. The schematic representations of the protein as fish, the ligand as triangles, and the diluting lipid as circles were borrowed from ref 13.

Almost all studies of 2D crystallization have been carried out under quiescent conditions (i.e., without fluid flow). However, the use of fluid dynamics has been suggested or implemented in two cases. In the first case, shear stress was applied to the monolayer by a rotating disk float that was used to measure the monolayer lateral rigidity.[7,13] In the second case, the use of a deep-channel flow geometry was suggested in order to enhance protein crystallization by controlling the spatial distribution of the proteins at the air/water interface and to introduce advection to overcome diffusion limits in the bulk.[14]

The effects of varying the ionic strength[12] and pH[16] on 2D crystallization are well established, but the effects of fluid motion have not been previously reported. We have discovered that fluid flow can indeed induce crystallization.

We investigated the effects of flow in an apparatus consisting of a stationary open cylinder driven by the constant rotation of the floor (Figure 1). The experimental apparatus consists of a precision-bore glass cylinder of radius $R = 2.5$ cm and height $H = 0.66$ cm. The cylinder is filled exactly to the top rim with an aqueous buffer at about 22 °C (kinematic viscosity $\nu = 0.01$ cm^2/s, which is essentially the same as that of water). The cylinder is held just above an optical glass floor whose constant rotation at Ω rad/s drives the flow. When nondimensionalized, the rotation rate is the Reynolds number $Re = \Omega R^2/\nu$. The system is driven with large inertia to just below the level at which the bulk flow becomes unstable to 3D perturbations. Specifically, we set $Re = 10^3$ (the critical Re for $^H/_R = 0.25$ with a nominally clean air/water interface is about 1450), at which a wide range of shear is imposed by the axisymmetric flow across the air/water interface. The bulk flow consists of two regions: for $r \lesssim 0.4R$ it is essentially in solid-body rotation, and for $r \gtrsim 0.4R$, it is an overturning flow advecting angular momentum from the rotating floor boundary layer up to the interface imparting a radial distribution of azimuthal shear to the monolayer. In the experiments, the crystals are visualized directly, as shown in Figure 1. Direct imaging of the interface illuminated by the forward scattering of a laser was found to be simple and effective because it avoids the need to label proteins for conventional fluorescence microscopy. Furthermore, direct imaging provides greater detail than Brewster angle microscopy. The very short pulse duration (5 ns) of the laser (New Wave Research, Solo-I) ensures sharp imaging even in flowing systems.

We found that when the interface is sheared, crystallization can be induced under conditions where none would occur without flow. Experiments were first performed in parallel using several identical quiescent systems so that various packing densities of the biotinylated lipid monolayer could be tested simultaneously. The systems consisted of wells with 25 mm diameter and 5 mm depth, machined in a Teflon block. A sapphire window was pressed into the bottom of each well, thus permitting laser-beam illumination from below, similar to the illumination used in the flow apparatus shown in Figure 1. The nonwetting nature of Teflon allows for the meniscus to form a few millimeters above the top of the well. For the preparation of the protein and ligand system, the experimental procedures of Gast's group[10,12,16] were followed with some modifications. [The wells and the cylinder are filled with a buffer solution with concentration of 50 mM (milli-molar) of NaH_2PO_4 and 500 mM of NaCl in Milli-Q filtered water (Millipore). A lipid mixture of Biotin-X-DHPE (Biotium) and DOPC (Avanti Polar Lipids) with 1:14 molar ratio (0.015 and 0.15 mg/ml, respectively) in 1:1 chloroform/hexane is spread on the aqueous buffer. Unlabeled streptavidin (saltfree, from *Streptomyces avidinii*; Sigma) reconstituted in deionized water at a concentration of 1 mg/ml is injected into the aqueous buffer to give a bulk protein concentration of 10 μg/ml. Crystallization generally occurs at room temperature (about 22 °C) and morphologies of streptavidin crystals are observed with the microscope.] For this system, with $4.0 < \mathrm{pH} < 4.5$, we were able to obtain crystals at surface pressures above 10 dynes/cm, consistent with the results of others.[17]

Figure 2a,b shows that in the absence of flow, for a system with a pH of 4.3, protein crystals with a wide-needle shape were found to grow in the expected range of surface pressure ($\pi = \sigma_{\mathrm{clean}} - \sigma$, where σ is the surface tension of the interface with a monolayer and σ_{clean} is the surface tension in the absence of a monolayer). Crystals were found to grow in both of the quiescent systems (Teflon wells and glass flow apparatus with the floor kept stationary) when the monolayer concentration exceeded about 1.5 mg/m^2. The corresponding surface pressure is greater than 10 dynes/cm. The photographs in Figure 2a,b show that below the critical monolayer concentration there are no crystals and only a few bright spots appear where clusters of protein molecules attach to the ligand sites at the interface. The consistency of the results obtained with the wells and with the flow apparatus with the stationary bottom shows that the shape of the meniscus and the volume/surface-area ratio do not have a measurable influence on the crystallization process. This observation is consistent with results showing the crystallization of proteins on lipid bilayers on highly curved vesicles.[18] In the quiescent system, crystals were generally observed after 1 to 4 h following the injection of protein into the bulk.

Subsequently, we discovered that by turning on the flow protein crystallization can be induced at lipid monolayer concentrations significantly below the threshold for crystallization in the absence of flow. Figure 2c shows that with flow, protein can be crystallized even at very low monolayer concentrations and correspondingly low surface pressures. The threshold surface pressure for crystallization with flow is below 1 dyn/cm, in contrast to a threshold of 10 dynes/cm without flow. These results were

(13) Lenne, P.-F.; Berge, B.; Renault, A.; Zakri, C.; Vénien-Bryan, C.; Courty, S.; Balavoine, F.; Bergsma-Schutter, W.; Brisson, A.; Grübel, G.; Boudet, N.; Komovalov, O.; Legrand, J.-F. *Biophys. J.* **2000**, *79*, 496−500.

(14) Drazek, L.; Legrand, J.-F.; Davoust, L. *J. Cryst. Growth* **2005**, *275*, 1467−1472.

(15) Brisson, A.; Bergsma-Schutter, W.; Oling, F.; Lambert, O.; Reviakine, I. *J. Cryst. Growth* **1999**, *196*, 456−470.

(16) Yatcilla, M. T.; Robertson, C. R.; Gast, A. P. *Langmuir* **1998**, *14*, 497−503.

(17) Ratanabanangkoon, P. Investing Streptavidin Crystallization on Lipid Monolayers and Bilayer Vesicles. Ph.D. Thesis, Stanford University, Stanford, CA, 2002.

(18) Ratanabanangkoon, P.; Gropper, R.; Merkel, M.; Sackmann, E.; Gast, A. P. *Langmuir* **2002**, *18*, 4270−4276.

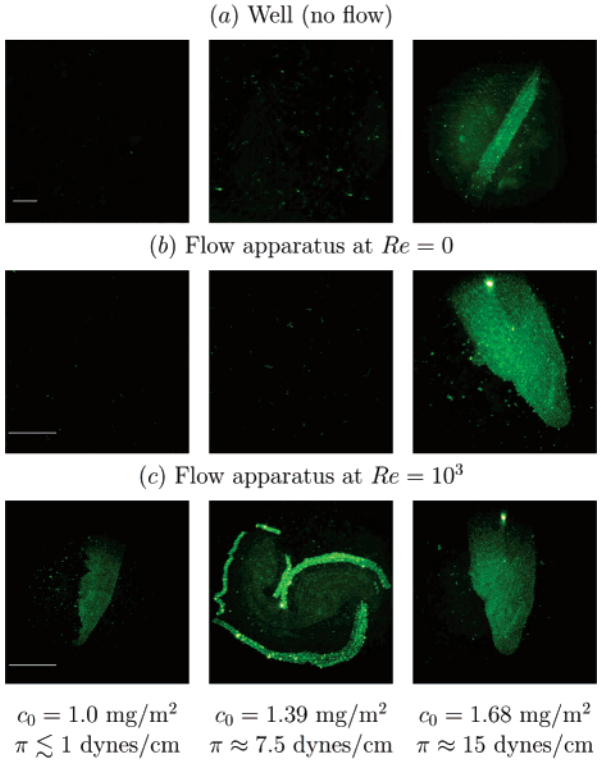

Figure 2. Protein crystallization with and without flow. (a) Quiescent Teflon wells in which crystallization occurs for monolayer surface concentrations corresponding to a surface pressure of >10 dynes/cm. Below the surface pressure threshold for crystallization (e.g., middle photograph at $\pi = 7.5$ dynes/cm), only clusters of streptavidin attached to the biotynalated lipid monolayer are observed, which appear as bright dots. (b) Flow apparatus with the floor kept stationary (i.e., $Re = 0$); crystallization occurred for essentially the same range of surface pressures as in the wells. (c) The threshold for protein crystallization is significantly reduced when the floor of the apparatus is rotating. In the $c_0 = 1.0$ and 1.39 mg/m^2 cases, no crystals were observed during the 2−4 h following the injection of protein into the bulk. However, within 15−20 min of the start of floor rotation, crystals were observed. In the $c_0 = 1.68$ mg/m^2 case, crystallization occurred in the absence of flow, as expected, and the photograph shows that the crystals remain robust in the presence of flow. The sharp edges observed in the large protein structures are due to their crystalline nature. The scale bars for each row are 250 μm.

reproduced on different days. The bright ring around the crystal in the $c_0 = 1.39$ mg/m^2 case is due to light scattering; such bright rings around the edge of the crystal have also been observed by others.[19]

A possible mechanism for flow-induced crystallization is that the overturning motion of the bulk flow, driven by the centrifugal acceleration generated by the rotation of the bottom floor, compresses the monolayer toward the center line of the cylinder. This results in an increase in the areal density of the ligand-bearing monolayer. In other monolayer systems, we have observed, both experimentally and computationally, such a compression of a monolayer by overturning bulk flow.[20,21] However, this does not seem to be the mechanism responsible for flow-enhanced crystallization, as explained below.

To elucidate the impact of flow on the monolayer, we simulated the system using the Navier−Stokes equations for the bulk flow coupled to a Boussinesq−Scriven surface model for an insoluble monolayer.[20] For the Marangoni stress in this model, we have measured the equation of state, relating surface tension to areal concentration of this monolayer consisting of a mixture of biotinylated lipid and diluting lipid. The measured equation of state together with the curve fit used in the numerical model is shown in Figure 3.

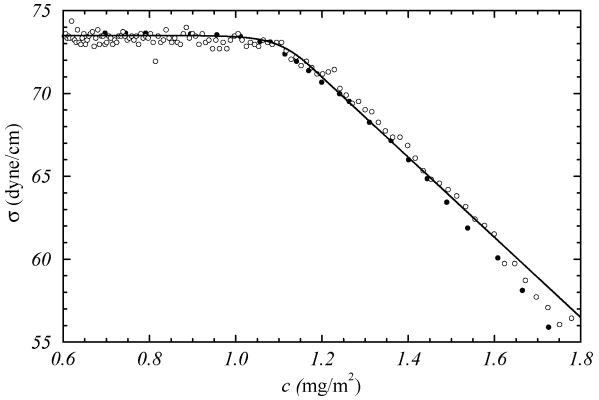

Figure 3. Measured equation of state for the monolayer (mixture of biotinylated lipid and diluting lipid), using quasi-static compression in a Langmuir trough, obtained on two different days using two different systems to digitize the output voltage from the Wilhelmy plate force transducer (○, ●). The curve fit (−) used in the numerical model is $\sigma = a_0 + a_1 \tanh(a_2 - a_3 c)$ for $c \leq a_2/a_3$ and $\sigma = a_0 + a_1(a_2 - a_3 c)$ for $c > a_2/a_3$, with $a_0 = 71.2$, $a_1 = 2.3$, $a_2 = 12.5$, and $a_3 = 10.5$.

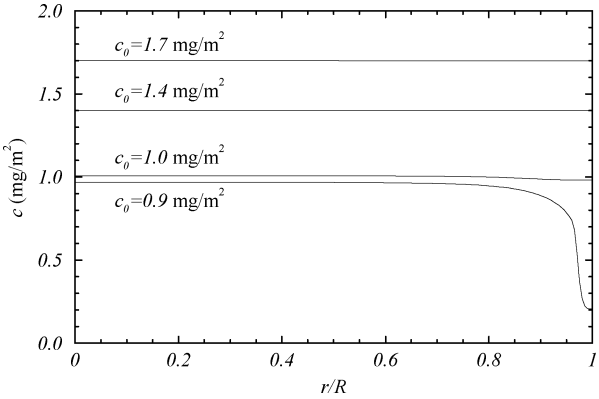

Figure 4. Computed monolayer concentrations at $Re = 10^3$ at steady state with the initial uniform monolayer concentration $c(r, t = 0) = c_0$ as indicated.

Figure 4 shows the computed concentration distribution $c(r)$ once the system has reached steady state (after about 15 floor rotations following an impulsive start from rest, corresponding to about 1 min in the physical experiment). Four different cases are shown corresponding to different initial uniform monolayer concentrations c_0. The case with the lowest initial concentration, $c_0 = 0.9$ mg/m^2, shows significant depletion of the monolayer near the cylinder wall due to advection by the overturning bulk flow. This does not take place for large c_0; the other three examples shown, $c_0 = 1.0$, 1.4, and 1.7 mg/m^2, correspond nominally to the three concentrations in the experiments presented in Figure 2. The equation of state in Figure 3 shows that for $c_0 \gtrsim 1.0$ mg/m^2 the Marangoni stress, which resists the compression of the monolayer and is proportional to $\partial\sigma/\partial c$, becomes significantly larger in magnitude. The numerical results presented in Figure 4 show that in essence, for all the crystallization experiments conducted (Figure 2c), the surface tension and the corresponding surface pressure are uniform along the interface. This rules out the compression of the monolayer as being a possible contributing mechanism for the observed flow-induced crystallization.

(19) Schief, W. R.; Dennis, S. R.; Frey, W.; Vogel, V. *J. Colloid Interface Sci.* **2000**, *171*, 75−86.
(20) Lopez, J. M.; Hirsa, A. *J. Colloid Interface Sci.* **2000**, *229*, 575−583.
(21) Hirsa, A. H.; Lopez, J. M.; Miraghaie, R. *J. Fluid Mech.* **2001**, *443*, 271−292.

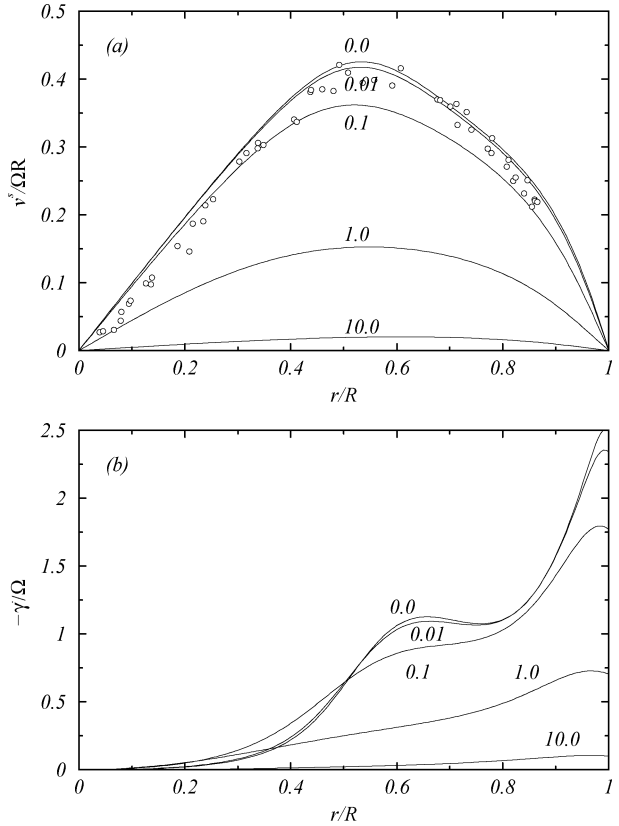

Figure 5. (a) Profiles of the azimuthal velocity at the air/water interface computed at $Re = 10^3$ for a radially stagnant monolayer model with surface shear viscosity $\mu^s/\mu R$ as indicated (−). The symbols are the experimentally measured velocity in a system with crystallized protein on a monolayer with $c_0 = 1.39$ mg/m^2. (b) Shear rate distribution at the interface, $\dot{\gamma}$, corresponding to the computed velocity profiles shown in part a.

Furthermore, for $c_0 > 0.9$ mg/m^2 the interface remains completely covered by the monolayer, and the radial component of velocity at the interface is zero at steady state. However, the monolayer is not immobilized; it is still flowing in the azimuthal direction.

Because monolayer compression does not occur, the only remaining rheological effect caused by the steady flow at the interface is due to azimuthal shearing of the monolayer. Figure 5a shows the computed azimuthal velocity at the interface for various values of surface shear viscosity $\mu^s/\mu R$ (nondimensionalized with the radius and the dynamic viscosity of the bulk μ) obtained using the radially stagnant monolayer model.[22]

The velocity at the air/water interface was measured for a system with a monolayer of concentration $c_0 = 1.39$ mg/m^2. The measurements were taken after the floor had been set to rotate for a few minutes. (The bulk flow reaches steady state in less than 1 min.) The duration of the measurements was about 1.5 h. The velocity was determined using double-exposed images of protein structures (crystals or clusters) attached to ligands in the monolayer; the displacement between the double-exposed image multiplied by the laser repetition rate (30 Hz) gives the velocity. For the measurements, a zoom setting of 2× on the microscope lens was used along with a 10× microscope objective, providing a 2 mm^2 field of view.

The measured profile correlates well with the numerical macroscale model data for cases with surface shear viscosity in the range of $\mu^s/\mu R \in (0.01, 0.1)$. Experimental data was obtained up to $r/R \approx 0.85$. (Light scattering from the cylinder wall prevents proper imaging of the protein at the interface for larger r.) The experimentally measured velocity profile shown in Figure 5a has a scatter of about 5%. Even with this relatively large scatter, it is clear that the interface is being sheared, primarily for $r/R >$ 0.4; for $r/R < 0.4$, the velocity profile is essentially linear, $v^s \propto r$, corresponding to solid body rotation. The shear in question is $\dot{\gamma} = r\partial(v/r)/\partial r$ evaluated at the interface. ($\dot{\gamma}$ profiles corresponding to the computed velocity profiles are shown in part b of the Figure.) The maximum shear occurs at the outermost radial region of the interface.

The present experiments show that a shearing flow can induce crystallization at conditions under which streptavidin would not crystallize on a biotinylated monolayer in the absence of flow. We have explored which macroscale flow mechanisms may be responsible for flow-induced crystallization. For the monolayer concentration range where crystallization is observed, the Marangoni stress is large enough to produce a negligible concentration gradient for the monolayer. Thus, there is no evidence of radial redistribution of the ligand-bearing monolayer by the flow. The numerical model results provide a clear macroscopic picture of the shear distribution at the interface, and the experimental measurements give essentially the same shear distribution. The crystals induced by the flow were observed to form for $r \geq 0.5R$ and up to the maximum radius of about $0.85R$ (where visualization was possible). For example, the left photograph in Figure 2a taken at a radius between $0.5R$ and $0.6R$ shows one of the earliest crystals to form a few minutes after the flow was started. Subsequently, other crystals were found to form at around that radius and larger, supporting the contention that the primary mechanism by which this flow system induces protein crystallization at the surface is strongly correlated to the shearing of the interfacial layer by the bulk flow. If indeed shear is the primary mechanism for flow-induced crystallization, the question then arises as to how it works. On one hand, the shear can preferentially order the ligands and any proteins attached to them at the interface. On the other hand, the shearing flow also provides vorticity normal to the interface and so results in the rotation of the proteins after they bind to the ligands (and prior to crystallization), thus allowing adjacent protein structures to click into place and form the crystals. This mechanism has to be present with or without flow.[15] These conjectured mechanisms warrant further investigation.

Acknowledgment. We are grateful to Alice Gast and Wolfgang Frey for sharing their insights on 2D crystallization in quiescent systems. This work was partially supported by the National Science Foundation through grants CTS0340768, CTS0340736, and DMS05052846.

LA063223X

(22) Hirsa, A. H.; Lopez, J. M.; Miraghaie, R. *J. Fluid Mech.* **2002**, *470*, 135−149.